International Scientific Conference 20 UNITECH 26

INTERNATIONAL SCIENTIFIC CONFERENCE
19-21 November 2026
GABROVO

# MEASUREMENT NOISE FILTERING AND HIDDEN CONTROL SIGNAL VARIANCE IN PIDD² CONTROL OF LTI SISO SYSTEMS

**Aleksandar Micić[1*], Djoko Bandjur[1], Aleksandar Žorić[1], Nikola Žorić[1]**

[1]*Faculty of Technical Sciences, Kneza Miloša 7, Kosovska Mitrovica, Serbia*
**Corresponding author: aleksandar.micic@pr.ac.rs*

**Abstract**
*Filtered PIDD² control can improve reference tracking of integrating plants, but its second derivative branch can convert small sensor noise into substantial actuator command variation that remains almost invisible at the plant output. This paper examines this hidden control effort problem using transfer function analysis. A two degree of freedom controller structure is adopted in which the proportional and integral terms process the reference, while filtered derivative actions operate in the measurement feedback path. Closed loop transfer functions are derived from the reference, plant input disturbance, and measurement noise to both the physical output and the controller output signal. A double integrator plant with an additional real pole is used as a representative electromechanical process. Second and third order realizations of the second derivative filter are compared using finite band noise indices, physical signal variances, reference tracking, and disturbance rejection. Simulation results show that an apparently smooth output can coexist with intensive actuator activity. Adding a third filter pole makes the second derivative branch strictly proper and reduces high frequency control signal variation while preserving useful transient performance and low frequency disturbance rejection.*

**Keywords:** PIDD² control, measurement noise, control signal variance, derivative filtering.

## INTRODUCTION

Derivative feedback is routinely used to shape the transient response of servo and motion control systems. A conventional PID controller introduces a velocity like term that increases damping; PIDD² control adds a second derivative term, often interpreted as filtered acceleration feedback. This extra degree of freedom can reduce overshoot and settling time, but an ideal $s^2$ operator is non causal and strongly amplifies high frequency sensor noise. A practical realization therefore requires explicit derivative filtering, and the filter order must be treated as a controller design parameter rather than as an implementation detail [1]–[5].

The relevant engineering risk is actuator side activity that is poorly visible in the measured plant output. Measurement noise is processed by the controller before the plant; consequently, a rapidly varying voltage, current, torque or valve command may be generated while plant inertia and actuator dynamics attenuate the corresponding output motion. The result can be increased RMS current, heating, acoustic excitation, wear, quantization cycling and saturation probability even when the output trace appears smooth. Noise assessment must therefore include both the noise to output and noise to control signal transfer functions [1]–[4].

For the filtered second derivative branch (D2F) defined below, the distinction between a second and a third order denominator is fundamental. With two filter poles the branch is proper but approaches a finite high frequency gain. With three poles it is strictly proper and its magnitude decays asymptotically as $1/\omega$, i.e. at $-20\ dB/dec$. The additional pole therefore attenuates high frequency control signal noise at the cost of extra phase lag, so filter bandwidth and second derivative gain must be selected jointly.

The controller structure is particularly relevant when the derivative terms have a clear physical interpretation as velocity and


*This is an open access article licensed under Creative Commons Attribution 4.0 International*
*Print ISSN: 1313-230X, Online ISSN: 3033-1404*

acceleration feedback. Examples include robot joint and electromechanical servo drives, precision positioning stages, and related motion systems; PIDD² control has also been experimentally demonstrated for synchronous generator automatic voltage regulation in a noisy laboratory environment [6]. The present results are obtained exclusively from transfer function analysis and numerical simulation of continuous time LTI SISO models with additive measurement noise over a prescribed finite frequency band. They therefore characterize the assumed model class and should not be interpreted as experimental validation or as a performance guarantee for nonlinear, sampled data, or saturating actuator systems.

## EXPOSITION

The design goal is to select a realizable two degree of freedom (2DOF) PIDD² structure that limits measurement noise induced actuator activity without sacrificing useful transient performance. The study separates reference and measurement feedback paths, derives transfer functions from reference, plant input disturbance and sensor noise to both physical output and control signal, introduces finite band noise measures, and compares second and third order D² filtering under identical controller gains and time constants.

The hypothesis is that a third order D² filter (F3) retains the transient benefits of PIDD² control while reducing control signal noise variance relative to the second order F2 realization. Since the noise to output path contains the attenuating plant, intensive actuator fluctuations may remain almost invisible at the output. F3 is therefore compared with F2 for noise attenuation and with the PIDD baseline for overshoot and settling time; these are distinct benchmarks.

Let $P(s) = B(s)/A(s)$ denote the plant. The symbols $r$, $d_i$, $u$, $y$, and $n$ denote the reference, plant input disturbance, controller output, physical plant output, and additive sensor noise, respectively. The measured signal is $y_m = y + n$, and the actual plant input is $u + d_i$. The adopted controller has a two degree of freedom PIDD² structure: the reference operator shapes the set point response, whereas the feedback operator closes the measurement loop. The control law is

$$y(s) = P(s)[u(s) + d_i(s)],$$
$$u(s) = C_r(s)r(s) - C_y(s)y_m(s) \qquad (1)$$

$$C_r(s) = bK_p + \frac{K_i}{s},$$
$$C_y(s) = K_p + \frac{K_i}{s} + D_1(s) + D_{2,q}(s) \qquad (2)$$

$$D_1(s) = \frac{K_{d1}s}{(1+T_{f1}s)^2},$$
$$D_{2,q}(s) = \frac{K_{d2}s^2}{(1+T_{f2}s)^q}, \quad q \in 2,3 \qquad (3)$$

The reference operator contains only proportional and integral actions. The set point weight $b$ shapes the proportional response to reference changes, while integral action provides low frequency accuracy and constant load rejection. In the feedback path, $D^1$ acts as filtered velocity feedback and $D^2$ as filtered acceleration feedback. Because both derivative branches act on the measured output $y_{\mathrm{m}}$ rather than on $r$, a step reference does not produce derivative kick on output. The repeated poles in (3) regularize the derivative operators and limit high frequency noise transmission. By setting $K_{d2} = 0$, while $b$, $K_p$, $K_i$, $K_{d1}$and $T_{f1}$ are kept unchanged, we obtain PIDD controller

$$u_{PIDD}(s) = K_p[br(s) - y_m(s)] + \frac{K_i}{s}[r(s) - y_m(s)] - \frac{K_{d1}s}{(1+T_{f1}s)^2}y_m(s), K_{d2} = 0. \qquad (4)$$

The closed loop system with the PIDD² controller is shown in Fig. 1.

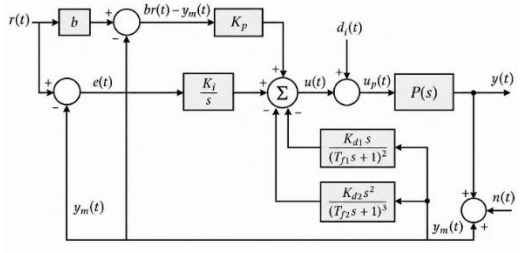



***Fig. 1.*** *Two degree of freedom (2DOF) PIDD² structure with filtered derivative feedback.*

Define the sensitivity and complementary-sensitivity functions as $S(s) = [1 + P(s)C_y(s)]^{-1}$ and $T(s) = P(s)C_y(s)S(s)$. The closed-loop transfer functions relevant to reference tracking and measurement-noise propagation are

$$H_{ry}(s) = P(s)C_r(s)S(s), \quad H_{ur}(s) = C_r(s)S(s) \tag{5}$$

$$H_{yn}(s) = -P(s)C_y(s)S(s) = -T(s), \quad H_{un}(s) = -C_y(s)S(s), H_{yn}(s) = P(s)H_{un}(s) \tag{6}$$

For a plant input disturbance, $H_{yd}(s) = P(s)S(s)$ and $H_{ud}(s) = -C_y(s)P(s)S(s) = -T(s)$. The two measurement noise paths additionally satisfy $H_{yn}(s) = P(s)H_{un}(s)$, $\frac{|H_{un}(j\omega)|}{|H_{yn}(j\omega)|} = \frac{1}{|P(j\omega)|}$ . (7)

The second relation in (7) explains the central effect: at frequencies where the plant magnitude is small, the controller may generate a large noise driven control signal while the resulting physical output motion remains negligible. Analyzing only output signal can therefore hide substantial actuator activity.

For a one sided measurement noise power spectral density per angular frequency, normalized such that its integral divided by $2\pi$ equals the input variance, the physical output or control signal variance is

$$\sigma_x^2 = \frac{1}{2\pi}\int_0^\infty |H_{xn}(j\omega)|^2\, \Phi_n(\omega)\, d\omega, x \in y, u \tag{8}$$

For a prescribed analysis band, the finite-band noise transmission integral and the associated band-averaged RMS gain are defined as

$$J_x = \int_{\omega_L}^{\omega_H} |H_{xn}(j\omega)|^2\, d\omega, \quad G_x = \sqrt{\frac{J_x}{\omega_H - \omega_L}}, \quad x \in y, u \tag{9}$$

The finite band integral is an accumulated squared transfer magnitude and is neither energy nor variance. The normalized RMS gain is directly interpretable; it is dimensionless when input and output have the same physical unit. In the simulations the excitation is modeled as band limited white measurement noise, meaning that its one sided power spectral density is constant over the selected frequency interval and zero outside it. For this model, output or control signal RMS is obtained by multiplying the corresponding band-averaged RMS gain by the input noise RMS.

The nominal plant used for the numerical study is

$$P(s) = \frac{1}{s^2(0.2s+1)} \tag{10}$$

At high-frequency the nominal plant magnitude decays approximately as $5/\omega^3$, so the control signal noise to output noise amplitude ratio grows approximately as $0.2\omega^3$; at $100\ rad/s$ it is about $2 \times 10^5$. For measurement noise the test band is $10 - 500\ rad/s$ and the RMS is 5 mV. The PIDD controller in (4) is compared with PIDD²-F2 and PIDD²-F3, which use $q = 2$ and $q = 3$ in (3), respectively, with all remaining parameters unchanged.

The reduced design starts from $P_0(s) = K_0/s^2$ with $K_0 = 1$, temporarily omitting the actuator pole, integral action and D² branch. For PD feedback $C_f(s) = K_p + K_{d1}s$, the characteristic equation $1 + P_0(s)C_f(s) = 0$ gives

$$s^2 + K_0K_{d1}s + K_0K_p = s^2 + 2\zeta\omega_n s + \omega_n^2 \tag{11}$$

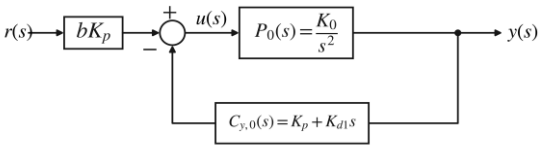



***Fig. 2.*** *Simplified system for deriving Equation (11).*

Matching coefficients in (11) gives $K_p = {\omega_n}^2/K_0$ and $K_{d1} = 2\zeta\omega_n/K_0$. With $\omega_n = 2$ rad/s, $\zeta = 0.70$ and $K_0 = 1$, one obtains $K_p = 4$ and $K_{d1} = 2.8$. With unity

reference weight $b = 1$, a unit step initially control signal $u(0^+) = 4$, within the prescribed limit. The complete model is used for all reported results.

The double integrator already provides zero steady state error for a reference step; integration mainly rejects a constant plant input disturbance. The deliberately slow time $T_i = 40$ s is a separate design choice, not a result of (11). It gives $K_i = K_p/T_i = 0.10$ and an approximate slow pole $-1/T_i = -0.025$ s$^{-1}$, with little influence on the dominant 2–4 s transient. Disturbance recovery is checked using the full model.

The first-derivative filter pole frequency $\omega_1 = 33.3$ rad/s was chosen well above $\omega_n = 2$ rad/s (ratio 16.7) to retain effective velocity feedback; hence $T_{f1} = 1/\omega_1 \approx 0.030$ s. Its squared denominator makes the D branch strictly proper. The D² filter pole was placed near the lower edge of the noise band: $\omega_2 = 8.33$ rad/s implies $T_{f2} = 1/\omega_2 \approx 0.120$ s. The stated frequencies are pole frequencies of the repeated first-order factors, not the $-3\,dB$ frequencies of the overall filters.

For F3, $K_{d2}$ and $T_{f2}$ were jointly screened using the complete closed loop: overshoot ≤8%, 2% settling time $\leq 3\,s$, and band averaged control signal noise gain $\leq 24$ over $10 - 500\,rad/s$. The selected pair $K_{d2} = 0.20$, $T_{f2} = 0.120$ s corresponds to the same $\omega_2 = 8.33$ rad/s stated above; $T_{f2}$ is not determined twice. F2 uses identical parameters except for D² filter order $q = 2$ instead of $q = 3$ and is retained as a comparison, although it fails some F3 design limits (Table 1).

Table 1 separates reference-transient quality from the noise-driven actuator cost.

*Table 1. Reference-response and band-limited measurement-noise results.*

| Structure | $M_p$ [%] | $t_s$ [s] | $\sigma_y^2$ [V²] / $\sigma_u^2$ [V²] |
|---|---|---|---|
| PIDD | 12.17 | 4.210 | 2.82×10⁻⁹ / 0.01282 |
| PIDD²-F2 | 9.56 | 2.636 | 4.74×10⁻⁹ / 0.02533 |
| PIDD²-F3 | 7.95 | 2.939 | 3.70×10⁻⁹ / 0.01390 |

The RMS output noise is 0.0688 mV (F2) and 0.0609 mV (F3), versus 159.16 and 117.89 mV RMS control signal noise, respectively. Independent transfer function and spectral calculations reproduce Table 1 within rounding. These values confirm that a nearly noise free plant output can conceal substantial actuator activity.

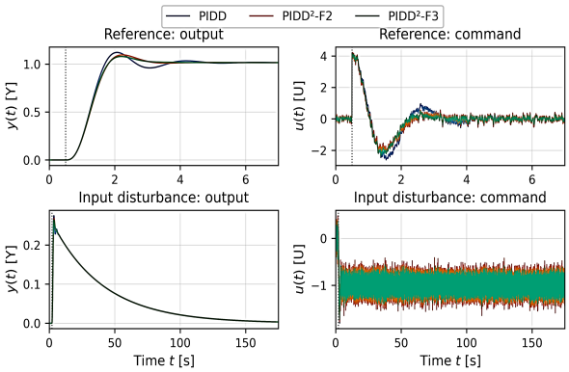



***Fig. 3.*** *Reference and input disturbance tests with measurement noise; PIDD = baseline (4).*

Figure 4 shows that output noise components remain small, whereas F2 causes the largest control signal fluctuations and F3 attenuates their high frequency part. Figure 3 confirms faster reference tracking than PIDD and comparable low-frequency disturbance rejection. Spectral variances are reproducible; exact random time traces depend on the particular noise realization.

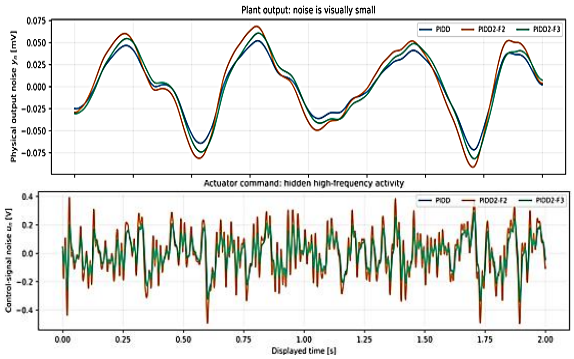



***Fig. 4.*** *Output and control signal noise: small output motion conceals large actuator/control signal variation.*

The comparison does not imply universal superiority of D² action. It shows that output only tuning is incomplete when derivative order increases: designs must also satisfy control signal variance, RMS current,

thermal loading, and saturation limits [1]–[4].

## CONCLUSION

Independent calculations confirm all Table 1 overshoots, 2% settling times and noise variances within rounding. A nearly noise free output may nevertheless conceal substantial actuator control signal noise. Relative to F2, F3 cuts control signal noise variance from 0.02533 to 0.01390 $V^2$ (45.1%), yet it remains 8.4% above the PIDD baseline (0.01282 $V^2$). In return, F3 reduces overshoot (12.17% to 7.95%) and 2% settling time (4.210 to 2.939 s) relative to PIDD. Thus F3 provides a tracking/noise compromise, not universally minimum control signal noise.

The additional $D^2$ filter pole makes the second derivative branch, but not the entire controller, strictly proper. The reported evidence is simulation based and limited to a continuous time LTI plant with band limited white measurement noise. It demonstrates the structural filtering mechanism and the associated tracking/noise tradeoff within that model class, but it does not constitute experimental validation or guarantee performance with nonlinear actuator dynamics, saturation, rate limits, sampling, or unmodeled dynamics. These effects should be examined in future simulation and experimental work.

## REFERENCE


[1] A. D. Micić, M. R. Mataušek, "Optimization of PID controller with higher-order noise filter," J. Process Control 24(5) (2014) 694–700.

[2] T. Hägglund, "A unified discussion on signal filtering in PID control," Control Eng. Pract. 21(8) (2013) 994–1006.

[3] V. Romero Segovia, T. Hägglund, K. J. Åström, "Measurement noise filtering for common PID tuning rules," Control Eng. Pract. 32 (2014) 43–63.

[4] B. Kristiansson, B. Lennartson, "Evaluation and simple tuning of PID controllers with high-frequency robustness," J. Process Control 16(2) (2006) 91–102.

[5] M. Huba, D. Vrančić, P. Bisták, "PID control with higher order derivative degrees for IPDT plant models," IEEE Access 9 (2021) 2478–2495.

[6] S. Veinović, D. Stojić, L. Ivanović, "Optimized PIDD2 controller for AVR systems regarding robustness," Int. J. Electr. Power Energy Syst. 145 (2023) 108646.